Eur. Phys. J. C (2014) 74:2998
DOI 10.1140/epjc/s10052-014-2998-9

THE EUROPEAN PHYSICAL JOURNAL C

Regular Article - Theoretical Physics

Impulsive cylindrical gravitational wave: one possible radiative form emitted from cosmic strings and corresponding electromagnetic response

Hao Wen[1,2], **Fangyu Li**[1,a], **Zhenyun Fang**[1], **Andrew Beckwith**[1]

[1] Department of Physics, Chongqing University, Chongqing 400044, People's Republic of China
[2] College of Materials Science and Engineering, Chongqing University, Chongqing 400044, People's Republic of China

Received: 30 March 2014 / Accepted: 25 July 2014 / Published online: 20 August 2014

Abstract The cosmic strings (CSs) may be one type of important source of gravitational waves (GWs), and it has been intensively studied due to its special properties such as the cylindrical symmetry. The CSs would generate not only usual continuous GWs, but also impulsive GWs that bring about a more concentrated energy and consist of different GW components, broadly covering low-, intermediate- and high-frequency bands simultaneously. These features might underlie interesting electromagnetic (EM) responses to these GWs generated by the CSs. In this paper, with novel results and effects, we firstly calculate the analytical solutions of perturbed EM fields caused by the interaction between impulsive cylindrical GWs (which would be one of possible forms emitted from CSs) and background celestial high magnetic fields or widespread cosmological background magnetic fields, by using the exact form of the Einstein–Rosen metric rather than the planar approximation usually applied. The results show that perturbed EM fields are also in the impulsive form in accordant to the GW pulse, and the asymptotic behaviors of the perturbed EM fields are fully consistent with the asymptotic behaviors of the energy density, energy flux density, and Riemann curvature tensor of the corresponding impulsive cylindrical GWs. The analytical solutions naturally give rise to the accumulation effect (due to the synchro-propagation of perturbed EM fields and the GW pulse, because of their identical propagating velocities, i.e., the speed of light), which is proportional to the $\sqrt{\text{distance}}$. Based on this accumulation effect, in consideration of very widely existing background galactic–extragalactic magnetic fields in all galaxies and galaxy clusters, we for the first time predict potentially observable effects in the region of the Earth caused by the EM response to GWs from the CSs.

[a] e-mail: fangyuli@cqu.edu.cn

1 Introduction

Over the past century, direct detection of gravitational waves (GWs) has been regarded as one of the most rigorous and ultimate tests of general relativity, and it has always been deemed as of significant urgency and attracting extensive interest, by use of various observation schemes aiming on multifarious sources. Recently, the detection of the B-mode polarization of the cosmic microwave background has been reported [1], and once this result obtains complete confirmation, it must be a great encouragement for this goal of GW detection.

Different from the usual GW origins, we specially focus on another important GW source, namely, the cosmic strings (CSs), a kind of axially symmetric cosmological body, which has been intensively researched [2–13] in past decades, also as regards issues related to impulsive GWs [14–19] and continuous GWs [20–22]. CSs are one-dimensional objects that may have been formed in the early universe as the linear defects during a symmetry-breaking phase-transition [23–25], so it represents an infinitely long line source that would emit cylindrical GWs [26,27]. Because of these particularities, although the existence of the CSs has not been exactly concluded so far, GWs produced by the CSs already have attracted attention and several efforts of observation have been made by some major laboratories or projects, such as ground-based GW detectors [28–30] and a proposed space detector [31,32] in low- or intermediate-frequency bands.

Actually, the GWs generated by CSs could have a quite wide spectrum [3–6,33–35] even over 10^{10} Hz [7,21,34]. Due to the cylindrical symmetrical property and the broad frequency range of these GWs, it is very interesting to consider the interaction between the EM system and the cylindrical GWs from CSs, because the EM system could be quite suitable to reflect the particular characteristics of

cylindrical GWs for many reasons: the EM systems (natural or in laboratory) widely occur (e.g. celestial and cosmological background magnetic fields); the GW and EM signals have identical propagating velocity, thus leading to a spatial accumulation effect [36–38]; the EM system is generally sensitive to the GWs in a very wide frequency range (especially suitable to the impulsive form because the pulse comprises different GW components among broad frequency bands), and so on.

In this paper we study the perturbed EM fields caused by the interaction between the EM system and the impulsive cylindrical GWs which could be emitted from the CSs and propagate through the background magnetic field [39,40]; based on the rigorous Einstein–Rosen metric [41,42] (unlike usual planar approximation for weak GWs), analytical solutions of this perturbed EM fields are obtained, by solving second order non homogeneous partial differential equation groups (from electrodynamical equations in curved spacetime).

Interestingly, our results show that the acquired solutions of perturbed EM fields are also in the form of a pulse, which is consistent to the impulsive cylindrical GW; and the asymptotic behavior of our solutions are in accordant to the asymptotic behavior of the energy-momentum tensor and the Riemann curvature tensor of the cylindrical GW pulse. This confluence greatly supports the reasonableness and self-consistence of acquired solutions.

Due to the identical velocities of the GW pulse and perturbed EM signals, the perturbed EM fields will be accumulated within the region of background magnetic fields, similarly to previous research results [36–38]. Particularly, this accumulation effect is naturally reflected by our analytical solutions, and the result is derived that the perturbed EM signals will be accumulated by a term with the square root of the propagating distance, i.e. $\propto \sqrt{\text{distance}}$. Based on this accumulation effect, we first predict the possibly observable effects on the Earth (direct observable effect) or the indirectly observable effects (around a magnetar), caused by EM response to the cylindrical impulsive GWs, in the background galactic–extragalactic magnetic fields ($\sim 10^{-11}$ to 10^{-9} Tesla within 1 Mpc [43] in all galaxies and galaxy clusters) or strong magnetic surface fields of the magnetar [44] ($\sim 10^{11}$ Tesla or even higher).

It should be pointed out that CSs produce not only the usual continuous GWs [20–22], but also impulsive GWs which have held a special fascination for researchers [14–19] (e.g., the 'Rosen'-pulse is believed to transfer energy from the source of CSs [17]). In this paper, we will specifically focus on the impulsive cylindrical GWs, and we will discuss issues relevant to the continuous form in works done elsewhere. Some major reasons for this consideration include:

1. The impulsive GWs come with a very concentrated energy to give a comparatively high GW strength. In fact, this advantage is also beneficial to the detection by Adv-LIGO or LISA, eLISA (they may be very promising for GWs in the intermediate band ($\nu \sim 1$ to $1,000$ Hz) and low-frequency bands (10^{-6} to 10^{-2} Hz), and it is possible to directly detect the continuous GWs from the CSs). The narrow width of the GW pulse gives rise to greater proportion of energy distributed in the high-frequency bands (e.g. GHz band), and it is already out of the aimed frequency range of Adv-LIGO or LISA. However, the EM response could be suitable to these GWs with high-frequency components.
2. By Fourier decomposition, a pulse actually consists of different components of GWs over a very wide frequency range covering the low-, intermediate- and high-frequency signals simultaneously; these rich components make it particularly well suited to the EM response, which is generally sensitive to broad frequency bands.
3. The exact metric of impulsive cylindrical GW underlying our calculation, has already been derived and developed in previous works (by Einstein, Rosen, Weber and Wheeler [41,42,45,46]), to provide a dependable and ready-made theoretical foundation.

The plan of this paper is as follows. In Sect. 2, the interaction between impulsive cylindrical GWs and background magnetic field is discussed. In Sect. 3, analytical solutions of the perturbed EM fields are calculated. In Sect. 4, physical properties of the obtained solutions are in detail studied and demonstrated. In Sect. 5, EM response to the GWs in some celestial and cosmological conditions, and relevant potentially observable effects are discussed. In Sect. 6, asymptotic physical behaviors of the perturbed EM fields are analyzed with comparisons to asymptotic behaviors of the GW pulse. In Sect. 7, the conclusion and discussion are given, with both theoretical and observational perspectives for possible future subsequent work along these lines.

2 Interaction of the impulsive cylindrical GW with background magnetic field: a probable EM response to the GW

In Fig. 1, the EM perturbation caused by cylindrical impulsive GWs within the background magnetic field is portrayed. Here, the CS (along z axis) represents a line-source which produces GWs with cylindrical symmetry, and the impulsive GWs emitted from this CS propagate outwards in different directions, so we can chose one specific direction (the x direction, perpendicular to the CS; see Fig. 1) to focus on. In the interaction region near axis (symmetrical axis of the CS), a static (or slowly varying quasi-static) magnetic

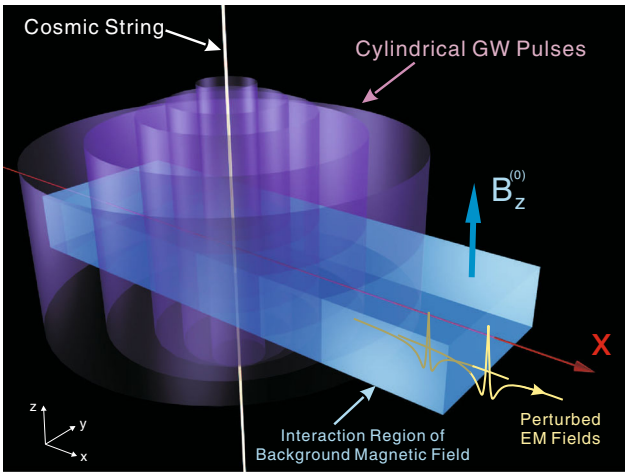

Fig. 1 Interaction between cylindrical impulsive GWs and background magnetic field. The cosmic string (alone z axis) is emitting GW pulses propagating outwards perpendicularly to the CS, and we only focus on the EM perturbation in the x direction specifically, the same hereinafter. The GW pulses will perturb the background magnetic field $B_z^{(0)}$ (pointing to the z axis) and produce the perturbed EM fields propagating in the x direction

field $B_z^{(0)}$ is existing as an interactive background pointing to the z direction. According to electrodynamical equations in curved spacetime [39,40], these cylindrical GW pulses will perturb this background magnetic field, and lead to perturbed EM fields (or in quantum language, signal photons) generated within the region of background magnetic field; then the perturbed EM fields simultaneously and synchronously propagate in the identical direction to the impulsive GWs along the x-axis.

As aforementioned in Sect. 1, the cosmic strings could generate impulsive GWs [14–19] with broad frequency bands [3–7,21,33,34]. The key profiles of impulsive GWs are the pulse width 'a', the amplitude 'A' and its specific metric. Here, for convenience and clarity, we select the Einstein–Rosen metric to describe the cylindrical impulsive GWs. This well-known metric initially derived by Einstein and Rosen based on general relativity [41,42,47] has been widely researched, as regards such pertinent issues as the energy-momentum pseudo-tensor [46–50]; its concise and succinct form could be advantageous to reveal the impulsive and cylindrical symmetrical properties of GWs. Using the cylindrical polar coordinates (ρ, φ, z) and time t, the Einstein–Rosen metric of the general form of cylindrical GW can be written as [41,42,45] ($c = 1$ in natural units)

$$ds^2 = e^{2(\gamma-\psi)}(dt^2 - d\rho^2) - e^{-2\psi}\rho^2 d\varphi^2 - e^{2\psi}dz^2; \quad (1)$$

then the contravariant components of the metric tensor $g^{\mu\nu}$ are

$$g^{00} = e^{2(\psi-\gamma)}, g^{11} = -e^{2(\psi-\gamma)},$$
$$g^{22} = -e^{2\psi}, g^{33} = -e^{-2\psi}. \quad (2)$$

and we have

$$\sqrt{-g} = e^{2(\gamma-\psi)} \quad (3)$$

here, the ψ and γ are functions of the distance ρ (which will be denoted as 'x' in the coordinates after this section) and the time t [41,42,45–47]. For the cylindrical impulsive GWs, a reasonable and well-known form is the Weber–Wheeler (W-W) solution [45,46], namely:

$$\psi(\rho, t) = A\left\{\frac{1}{[(a-it)^2+\rho^2]^{\frac{1}{2}}} + \frac{1}{[(a+it)^2+\rho^2]^{\frac{1}{2}}}\right\}, \quad (4)$$

$$\gamma(\rho, t) = \frac{A^2}{2}\left\{\frac{1}{a^2} - \frac{\rho^2}{[(a-it)^2+\rho^2]^2} - \frac{\rho^2}{[(a+it)^2+\rho^2]^2} - \frac{t^2+a^2-\rho^2}{a^2[t^4+2t^2(a^2-\rho^2)+(a^2+\rho^2)^2]^{\frac{1}{2}}}\right\}, \quad (5)$$

where A and a are corresponding to the amplitude and pulse width of the cylindrical impulsive GW, respectively.

3 The perturbed EM fields produced by the impulsive cylindrical GWs in the background magnetic fields

When the cylindrical impulsive GWs described in Sect. 2 [Eqs. (1) to (5)] propagate through the interaction region with background magnetic field $B_z^{(0)}$, perturbed EM fields will be generated. In this section, we will formulate a detailed calculation on the exact forms of the perturbed EM fields. Notice that the word 'exact' here means that we utilize the rigorous metric of cylindrical impulsive GW (Eq. 1) which keeps the cylindrical form, rather than the planar approximation usually used for weak fields as considered by the linearized Einstein equation. Nonetheless, the cross section of the interaction between background magnetic field and the GW pulse is still very small, so the consideration of perturbation theory is reasonably suited to handle this case, and as commonly accepted, some high order infinitesimals can be ignored. However, manipulating without using the perturbation theory and without any sort of approximation to seek absolutely strict results is also very interesting topic, and we would investigate such issues in other works. Therefore, the total EM field tensor $F_{\alpha\beta}$ can be expressed as two parts: the background static magnetic field $F^{(0)}_{\alpha\beta}$, and the perturbed EM fields $F^{(1)}_{\alpha\beta}$ caused by the incoming impulsive GW; Because of the cylindrical symmetry, it is always possible to describe the EM perturbation effect at the plane of $y = 0$ (i.e., the x–z plane, by use of a local Cartesian coordinate system, see Fig. 1, and the 'x' here substitutes for the distance ρ in Eqs.

(4) and (5)), then $F_{\alpha\beta}$ can be written as

$$F_{\alpha\beta} = F^{(0)}_{\alpha\beta} + F^{(1)}_{\alpha\beta} = \begin{pmatrix} 0 & E^{(1)}_x & E^{(1)}_y & E^{(1)}_z \\ -E^{(1)}_x & 0 & (-B^{(0)}_z - B^{(1)}_z) & B^{(1)}_y \\ -E^{(1)}_y & (B^{(0)}_z + B^{(1)}_z) & 0 & -B^{(1)}_x \\ -E^{(1)}_z & -B^{(1)}_y & B^{(1)}_x & 0 \end{pmatrix}. \tag{6}$$

Then, using the electrodynamical equations in curved spacetime:

$$\nabla_\nu F^{\mu\nu} = \frac{1}{\sqrt{-g}} \frac{\partial}{\partial x^\nu} [\sqrt{-g} g^{\mu\alpha} g^{\nu\beta} (F^{(0)}_{\alpha\beta} + F^{(1)}_{\alpha\beta})] = 0,$$
$$\nabla_\alpha F_{\mu\nu} + \nabla_\nu F_{\alpha\mu} + \nabla_\mu F_{\nu\alpha} = 0,$$
$$\text{where } F^{(0)}_{12} = -F^{(0)}_{21} = -B^{(0)}_z = -B^{(0)} \tag{7}$$

together with Eqs. (1)–(6), we have

$$\mu = 0 \Rightarrow 2(\gamma_x - \psi_x) E^{(1)}_x - \frac{\partial E^{(1)}_x}{\partial x} = 0, \tag{8}$$

$$\mu = 1 \Rightarrow 2(\psi_t - \gamma_t) E^{(1)}_x + \frac{\partial E^{(1)}_x}{\partial t} = 0, \tag{9}$$

$$\mu = 2 \Rightarrow 2\psi_t E^{(1)}_y + \frac{\partial E^{(1)}_y}{\partial t} + 2\psi_x (B^{(0)} + B^{(1)}_z) + \frac{\partial B^{(1)}_z}{\partial x} = 0, \tag{10}$$

$$\mu = 3 \Rightarrow 2\psi_t E^{(1)}_z + \frac{\partial E^{(1)}_z}{\partial t} - 2\psi_x B^{(1)}_y + \frac{\partial B^{(1)}_y}{\partial x} = 0, \tag{11}$$

$$\frac{\partial B^{(1)}_x}{\partial x} = 0, \quad \frac{\partial B^{(1)}_x}{\partial t} = 0,$$
$$\frac{\partial E^{(1)}_z}{\partial x} = \frac{\partial B^{(1)}_y}{\partial t}, \quad \frac{\partial E^{(1)}_y}{\partial x} = -\frac{\partial B^{(1)}_z}{\partial t}. \tag{12}$$

Here, γ_x, ψ_x, ψ_t, and γ_t stand for $\frac{\partial\gamma}{\partial x}$, $\frac{\partial\psi}{\partial x}$, $\frac{\partial\psi}{\partial t}$, and $\frac{\partial\gamma}{\partial t}$, and similarly hereinafter. So, by omitting second- and higher-order infinitesimal terms, it gives

$$\frac{\partial^2 E^{(1)}_y}{\partial x^2} - \frac{\partial^2 E^{(1)}_y}{\partial t^2} = 2\psi_{xt} B^{(0)}, \tag{13}$$

$$\frac{\partial^2 B^{(1)}_z}{\partial x^2} - \frac{\partial^2 B^{(1)}_z}{\partial t^2} = -2\psi_{xx} B^{(0)}. \tag{14}$$

Note that with Eqs. (8)–(12) and the initial conditions, we have

$$E^{(1)}_y\Big|_{t=0} = 0, \quad \frac{\partial E^{(1)}_y}{\partial t}\Big|_{t=0} = -2\psi_x|_{t=0} \cdot B^{(0)},$$
$$B^{(1)}_z\Big|_{t=0} = 0, \quad \frac{\partial B^{(1)}_z}{\partial t}\Big|_{t=0} = 0. \tag{15}$$

The other components, i.e., $E^{(1)}_x$, $B^{(1)}_x$ and $E^{(1)}_z$, $B^{(1)}_y$ have only null solutions. Non-vanishing EM components $E^{(1)}_y$ and $B^{(1)}_z$ are functions of x and t. To obtain their solutions, we need to solve the set of second-order non-homogeneous partial differential equations in Eqs. (13)–(15), and utilizing the d'Alembert formula, we can express the solutions in analytical form [51]:

$$E^{(1)}_y = \frac{1}{2}\int_{x-t}^{x+t} H(\xi)\mathrm{d}\xi + \frac{1}{2}\int_0^t \int_{x-(t-\tau)}^{x+(t-\tau)} F(\xi,\tau)\mathrm{d}\xi\mathrm{d}\tau, \tag{16}$$

$$B^{(1)}_z = \frac{1}{2}\int_0^t \int_{x-(t-\tau)}^{x+(t-\tau)} G(\xi,\tau)\mathrm{d}\xi\mathrm{d}\tau, \tag{17}$$

where

$$H(\xi) = -2\psi_\xi|_{t=0} \cdot B^{(0)},$$
$$F(\xi,\tau) = -2\psi_{\xi\tau} B^{(0)},$$
$$G(\xi,\tau) = 2\psi_{\xi\xi} B^{(0)}. \tag{18}$$

By the integral from Eq. (16), one finds

$$\frac{1}{2}\int_{x-t}^{x+t} H(\xi)\mathrm{d}\xi = -1\int_{x-t}^{x+t} \psi_\xi|_{t=0} \cdot B^{(0)}\mathrm{d}\xi = 2AB^{(0)}\left\{\frac{1}{[(x-t)^2+a^2]^{\frac{1}{2}}} - \frac{1}{[(x+t)^2+a^2]^{\frac{1}{2}}}\right\} \tag{19}$$

and, similarly,

$$\begin{aligned}\frac{1}{2}\int_0^t \int_{x-(t-\tau)}^{x+(t-\tau)} F(\xi,\tau)\mathrm{d}\xi\mathrm{d}\tau &= -AB^{(0)}\left\{\int_0^t \frac{\tau + ia}{[(x+t-\tau)^2+(a-it)^2]^{\frac{3}{2}}}d\tau\right. \\ &+ \int_0^t \frac{\tau - ia}{[(x+t-\tau)^2+(a+it)^2]^{\frac{3}{2}}}\mathrm{d}\tau \\ &- \int_0^t \frac{\tau + ia}{[(x-t+\tau)^2+(a-it)^2]^{\frac{3}{2}}}\mathrm{d}\tau \\ &\left.- \int_0^t \frac{\tau - ia}{[(x-t+\tau)^2+(a+it)^2]^{\frac{3}{2}}}\mathrm{d}\tau\right\}\end{aligned} \tag{20}$$

and

$$\begin{aligned}\frac{1}{2}\int_0^t \int_{x-(t-\tau)}^{x+(t-\tau)} G(\xi,\tau)\mathrm{d}\xi\mathrm{d}\tau &= -AB^{(0)}\left\{\int_0^t \frac{x+t-\tau}{[(x+t-\tau)^2+(a-i\tau)^2]^{\frac{3}{2}}}\mathrm{d}\tau\right. \\ &\left.+ \int_0^t \frac{x+t-\tau}{[(x+t-\tau)^2+(a+i\tau)^2]^{\frac{3}{2}}}\mathrm{d}\tau\right.\end{aligned}$$

$$-\int_0^t \frac{x-t+\tau}{[(x-t+\tau)^2+(a-i\tau)^2]^{\frac{3}{2}}}\mathrm{d}\tau - \int_0^t \frac{x-t+\tau}{[(x-t+\tau)^2+(a+i\tau)^2]^{\frac{3}{2}}}\mathrm{d}\tau\Bigg\}. \tag{21}$$

After a lengthy calculation of Eqs. (20) and (21), with combination of Eq. (19), the concrete form of the electric component of the perturbed EM fields can be deduced:

$$\begin{aligned}E_y^{(1)}(x,t) = 2AB^{(0)}&\left\{\frac{1}{[(x-t)^2+a^2]^{\frac{1}{2}}} - \frac{1}{[(x+t)^2+a^2]^{\frac{1}{2}}}\right.\\ &+\frac{a(x+t)\sin\left(\frac{1}{2}\theta_1\right)-a^2\cos\left(\frac{1}{2}\theta_1\right)}{[(x+t)^2+a^2][x^4+2x^2(a^2-t^2)+(a^2+t^2)^2]^{\frac{1}{4}}}\\ &+\frac{a^2}{[(x+t)^2+a^2]^{\frac{3}{2}}} - \frac{a^2}{[(x-t)^2+a^2]^{\frac{3}{2}}}\\ &\left.+\frac{a(x-t)\sin\left[\frac{1}{2}\theta_1\right]+a^2\cos\left[\frac{1}{2}\theta_1\right]}{[(x-t)^2+a^2][x^4+2x^2(a^2-t^2)+(a^2+t^2)^2]^{\frac{1}{4}}}\right\}\\ &+AB^{(0)}\left\{\frac{\cos\left[2\theta_2+\frac{1}{2}\theta_1\right]}{[x^4+2x^2(a^2-t^2)+(a^2+t^2)^2]^{\frac{1}{4}}}\right.\\ &-\frac{2\cos[2\theta_2]}{[(x-t)^2+a^2]^{\frac{1}{2}}}\\ &+\frac{[x^4+2x^2(a^2-t^2)+(a^2+t^2)^2]^{\frac{1}{4}}}{(x-t)^2+a^2}\cos\left[2\theta_2-\frac{1}{2}\theta_1\right]\\ &-\frac{\cos[2\theta_3-\frac{1}{2}\theta_1]}{[x^4+2x^2(a^2-t^2)+(a^2+t^2)^2]^{\frac{1}{4}}}+\frac{2\cos(2\theta_3)}{[(x+t)^2+a^2]^{\frac{1}{2}}}\\ &\left.-\frac{[x^4+2x^2(a^2-t^2)+(a^2+t^2)^2]^{\frac{1}{4}}}{(x+t)^2+a^2}\cos\left[2\theta_3+\frac{1}{2}\theta_1\right]\right\}.\end{aligned} \tag{22}$$

The same procedure, from Eqs. (14), (15), (17), and (18), will lead to the following, i.e. the concrete form of magnetic component of the perturbed EM fields can be derived to read:

$$\begin{aligned}&B_z^{(1)}(x,t)\\ &=-2AB^{(0)}\left\{\frac{(x+t)^2\cos\left(\frac{\theta_1}{2}\right)+(x+t)a\sin\left(\frac{\theta_1}{2}\right)}{[(x+t)^2+a^2][x^4+2x^2(a^2-t^2)+(a^2+t^2)^2]^{\frac{1}{4}}}\right.\\ &\quad-\frac{(x+t)^2}{[(x+t)^2+a^2]^{\frac{3}{2}}}\\ &\quad+\frac{(x-t)^2\cos\left(\frac{\theta_1}{2}\right)-(x-t)a\sin\left(\frac{\theta_1}{2}\right)}{[(x-t)^2+a^2][x^4+2x^2(a^2-t^2)+(a^2+t^2)^2]^{\frac{1}{4}}}\\ &\quad\left.-\frac{(x-t)^2}{[(x-t)^2+a^2]^{\frac{3}{2}}}\right\}\\ &\quad+AB^{(0)}\left\{\frac{\cos\left(2\theta_3-\frac{1}{2}\theta_1\right)}{[x^4+2x^2(a^2-t^2)+(a^2+t^2)^2]^{\frac{1}{4}}}\right.\\ &\quad-\frac{2\cos(2\theta_3)}{[(x+t)^2+a^2]^{\frac{1}{2}}}\\ &\quad+\frac{[x^4+2x^2(a^2-t^2)+(a^2+t^2)^2]^{\frac{1}{4}}}{(x+t)^2+a^2}\cos\left(2\theta_3+\frac{1}{2}\theta_1\right)\\ &\quad+\frac{\cos\left(2\theta_2+\frac{1}{2}\theta_1\right)}{[x^4+2x^2(a^2-t^2)+(a^2+t^2)^2]^{\frac{1}{4}}}-\frac{2\cos(2\theta_2)}{[(x-t)^2+a^2]^{\frac{1}{2}}}\\ &\quad\left.+\frac{[x^4+2x^2(a^2-t^2)+(a^2+t^2)^2]^{\frac{1}{4}}}{(x-t)^2+a^2}\cos\left(2\theta_2-\frac{1}{2}\theta_1\right)\right\},\end{aligned} \tag{23}$$

where the three angles used in Eq. (23) read

$$\theta_1 = \arctan\frac{2at}{x^2+a^2-t^2},\ \theta_2 = \arctan\frac{a}{x-t},\ \theta_3 = \arctan\frac{a}{x+t}. \tag{24}$$

The analytical solutions given above of the electric component $E_y^{(1)}(x,t)$ and the magnetic component $B_z^{(1)}(x,t)$ of the perturbed EM fields give a concrete description of the interaction between the GW pulse and the background magnetic field. Here, $E_y^{(1)}(x,t)$ and $B_z^{(1)}(x,t)$ are both functions of time t and coordinate x, with parameters 'A' (amplitude of the GW), 'a' (width of the GW pulse) and $B^{(0)}$ (background magnetic field). So, these solutions contain essential information inherited from their GW source (e.g. a cosmic string) and EM system (e.g., celestial or galactic–extragalactic background magnetic fields).

It is important to note that the analytical solutions Eqs. (22) and (23) of the perturbed EM field are also in the form of a pulse (see Fig. 2). Both Eqs. (22) and (23) are consistent with regards to the impulsive GWs. In Fig. 2a, this fact is explicitly revealed in that at a specific time t, the waveform of the electric field $E_y^{(1)}(x,t)$ exhibits a peak in magnitude. A similar situation also occurs as exhibited in Fig. 2b for the magnetic component of the perturbed EM fields.

On account of the cylindrical symmetry of the GW pulse, its source should be some one-dimensionally distributed object of very large scale, and according to current cosmological observations or theories, cosmic strings would almost certainly be the best candidate. Correspondingly, from the solutions, these impulsive peaks of perturbed EM fields are found to propagate outwards from the symmetrical axis of the CS, with their wavefronts also following a cylindrical manner (see Fig. 3), and meanwhile their levels gradually increase during this propagation process (due to the accumulation effect, which will be discussed later in this paper).

The analytical solutions Eqs. (22) and (23), which are in the impulsive form, bring us important key information and show the special nature of the perturbed EM fields, as well as various underlying physical properties, potentially

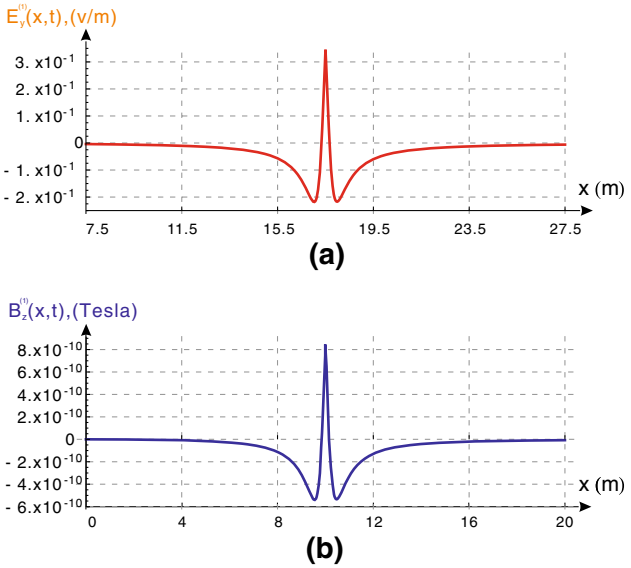

Fig. 2 Typical examples of electric and magnetic components of perturbed impulsive EM fields in the region near axis. According to Eq. (22), **a** a representative electric component $E_y^{(1)}(x,t)$ of the impulsive EM field produced by the interaction between cylindrical GW pulse (width $a = 0.4$ m, amplitude $h \sim 10^{-21}$; here we denote 'h' instead of 'A' as the amplitude in the SI units, similarly hereinafter) and higher background magnetic field (10^{11} Tesla, could be generated from celestial bodies [44], the same hereinafter). Here we assume $h \sim 10^{-21}$ (similarly in the figures below), and the detailed reason for this choice may be found in Sect. 5. In the same way, according to Eq. (23), **b** a typical magnetic component $B_z^{(1)}(x,t)$ of perturbed EM fields (with GW width $a = 0.4$ m, $h \sim 10^{-21}$) in the region of the near axis. Both electric and magnetic components of the perturbed impulsive EM fields are in the form of a pulse, consistent with the GW pulses. This figure is plotted assuming SI units

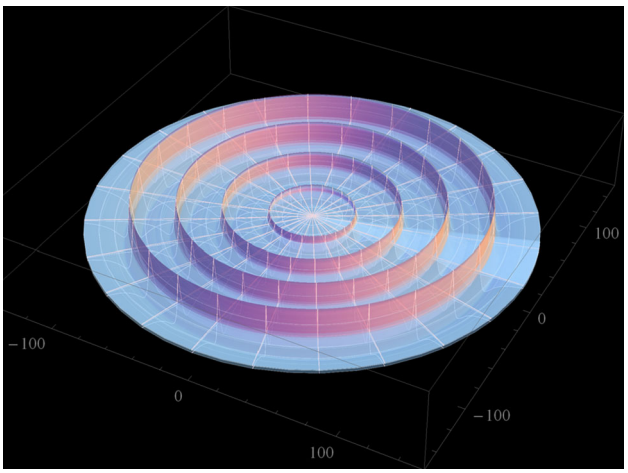

Fig. 3 Wavefronts of the perturbed EM fields in background magnetic field. The plot generated above is based upon Eq. (22), and it demonstrates the cylindrical wavefronts of the EM fields as perturbed by the cylindrical GW pulses

observable effects, and asymptotic behaviors. These aspects will consequently be analyzed and discussed in full in the following sections.

4 Physical properties of analytical solutions of the perturbed EM fields

With the analytical solutions of the perturbed EM fields as represented in the above section, some of their interesting properties may be studied in detail. For example, what is the relationship between the given width-amplitude of the perturbed EM fields and the width-amplitude of the GW pulse? Secondly, is there any accumulation effect (consistent with previous work in the literature on the EM respond to GWs) of the interaction between the GW pulses and the background magnetic field since the GWs and the perturbed EM fields share the same velocity (speed of light)? In addition we also ask what the spectrum is of the amplitude of the perturbed EM field and how it is related to the parameters of the corresponding GW pulse. For convenience, we use SI units in this section and Sect. 5. The details are as follows:

1. The relationship between the parameters of the GW pulse and the impulsive features of the perturbed EM field.
   From Eq. (22), it is simply deduced that the amplitude h (here 'h' is written in place of 'A' as the amplitude in SI units) of the GW pulse and the background magnetic field, $B^{(0)}$, contribute linear factors for the perturbed EM field which we designate in this paper as $E_y^{(1)}(x,t)$. So $E_y^{(1)}(x,t)$ varies according to h proportionally (see Fig. 4b). However, the width 'a' of a GW pulse plays a more complex role in Eq. (22), but we find that the width 'a' is still positively correlated to the width of the perturbed EM fields, i.e., a smaller width of the GW pulse leads to a smaller width of the perturbed EM field (see Fig. 4a), and the EM pulse with a narrower peak is found to have a larger strength and a more concentrated energy.
2. Propagating velocity of perturbed EM pulses.
   The information as regards the propagating velocity of the GW as the speed of light is naturally included in the definition of the metric (Eqs. (1)–(5)). In the same way, EM pulses caused by the GW pulse also are propagating at the speed of light due to EM theory in free space (but also in curved spacetime) [39,40]. For intuitive representation, we exhibit this property in Fig. 5, which illustrates the exact given field contours of $E_y^{(1)}(x,t)$ at different times from $t = 0$ to $t = \frac{20}{c}$ s.
3. Accumulation effect due to the identical propagating velocity of EM pulses and GW pulse.
   As mentioned above, we see that the perturbed EM fields propagate at the speed of light synchronously with the GW pulse; then the perturbed EM fields caused by the interaction between GW pulse and background magnetic field will accumulate. So, in the region with a given back-

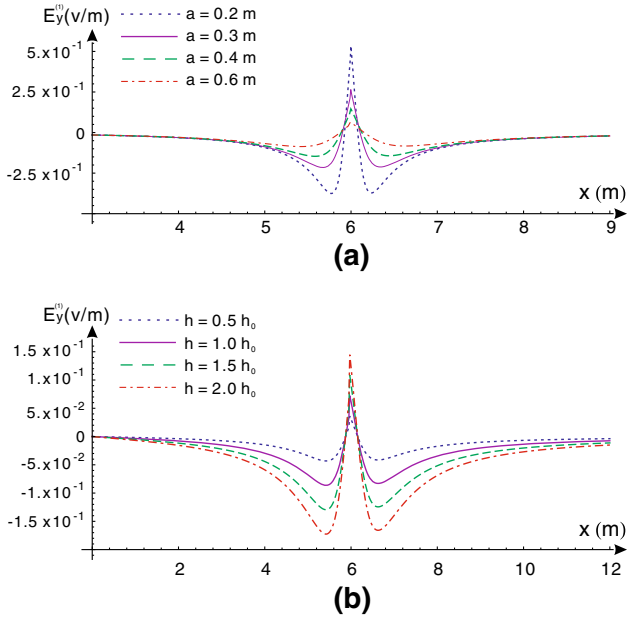

Fig. 4 EM fields perturbed by the GW pulses with different widths and amplitudes. Here, **a** the electric components of EM fields perturbed by the GW pulses with different pulse widths (from $a = 0.2$ to 0.6 m, given the same amplitude $\sim 10^{-21}$ in the region near axis). It is indicated that a larger width of the GW pulse gives rise to a larger width of the corresponding perturbed EM pulse, but it also results in a flatter waveform with less concentrated energy. **b** The impact of different amplitudes ($h = 0.5$ to 2 h_0, $h_0 \sim 10^{-21}$) of the GW pulses with the same width, and explicitly we find that higher amplitudes of the GW pulse lead to a correspondingly greater amplitude of the perturbed EM field. Note that the growth of the amplitude of GW does not influence the width of the perturbed EM pulse

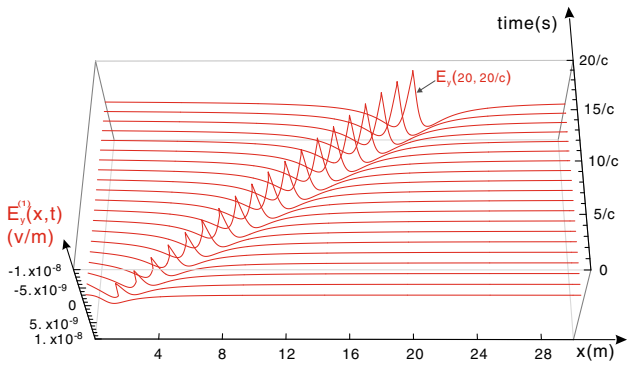

Fig. 5 Perturbed EM field propagates at the speed of light. This plot visually displays the propagating process of a typical perturbed EM pulse from $t = 0$ to $t = \frac{20}{c}$ s, which is linearly moving from $x = 0$ m to $x = 20$ m during this period. That is, the speed of propagation of the perturbed EM pulse is $20/\frac{20}{c} = c$, the same as the speed of light

ground magnetic field, the strength of the perturbed EM pulse will gradually rise (see Fig. 6) until it leaves the boundary of the background magnetic field. Except for the reason of their synchronous propagation, the accumulation should also be determined by another fact: that the energy flux of impulsive cylindrical GW will decay as $1/distance$ (or $\sim 1/x$ on light cone, see Eq. (33), so the strength of impulsive cylindrical GW will decay as $1/\sqrt{\text{distance}}$), and their composite accumulation effect is proportional to $\sqrt{x}$ (see Eq. (28)). In Fig. 6, we can also find that the accumulation effect is conspicuous, and for diverse cases of perturbed EM fields with different parameters of width of the GW pulses (see Fig. 6), this phenomenon always appears generally, and in Fig. 7, the contours of perturbed EM fields (electric component), in different positions, also explicitly demonstrate the accumulated perturbed impulsive EM fields, during their propagating away from the GW source.

4. Amplitude spectra of perturbed EM fields influenced by amplitude of the GW pulse.
   As mentioned above, the perturbed impulsive EM field is comprised of components with very different frequencies among a wide band. Shown in Fig. 8, the Fourier transform of the field $E_y^{(1)}(x, t)$ in the frequency domain illustrates the distribution of the amplitude spectrum. Although this spectrum decreases as it approaches the high-frequency range, it still remains available at a level in the neighborhood of the GHz band. Overall, it is indicated that (see Fig. 8) the level of the spectrum is proportional to the amplitude of the GW pulse, which causes the perturbed EM fields, commonly among entire frequency bands.
5. Amplitude spectra of perturbed EM fields influenced by the width of GW pulse.
   In contrast to what happens to the GW amplitude h, the width of the GW pulse acts so as to impact the distribution of the amplitude spectra of the perturbed EM fields, apparently in a nonlinear manner (see Fig. 9). The narrow width of the GW pulse will lead to a rich spectrum in the high-frequency region, such as the GHz band, as exemplified by the upper-left subplot of Fig. 9, where the width of the GW pulse is 0.1 m, and hence the sum of the energies of the spectral components from 1 to 9.9 GHz is approximately 24.5 % of the total energy. Once the width rises, as shown in the other three subplots in Fig. 9, gradually the amplitude spectra will decrease in the high-frequency domain. This property elucidates why the smaller width of the GW pulse would more likely cause a stronger effect of the EM response especially in the high-frequency band, and this phenomenon is generally appearing in the wide continuous parameter range (see Fig. 10).

To summarize, based on the above interesting properties, we can argue that: the amplitude of the GW pulse will proportionally influence the level and overall amplitude spectrum

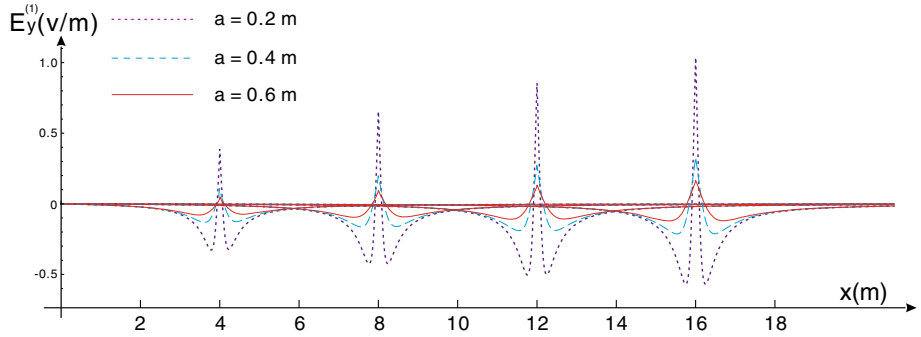

Fig. 6 Accumulation effect of the perturbed EM fields. When the impulsive EM fields propagate from $x = 0$, at different positions of $x = 4, 8, 12, 16$ m in the region near axis (at different times, t, amplitude $h \sim 10^{-21}$, background magnetic field $\sim 10^{11}$ Tesla), the amplitude of the EM fields will then increase, because the perturbed EM fields propagate synchronously with the GW pulse with the identical velocity of the speed of light; then the interaction between the GW pulse and background magnetic field will be finally accumulated. Here, this figure shows that this accumulation phenomenon commonly appears in all cases with different widths from 0.2 to 0.6 m of the GW pulses

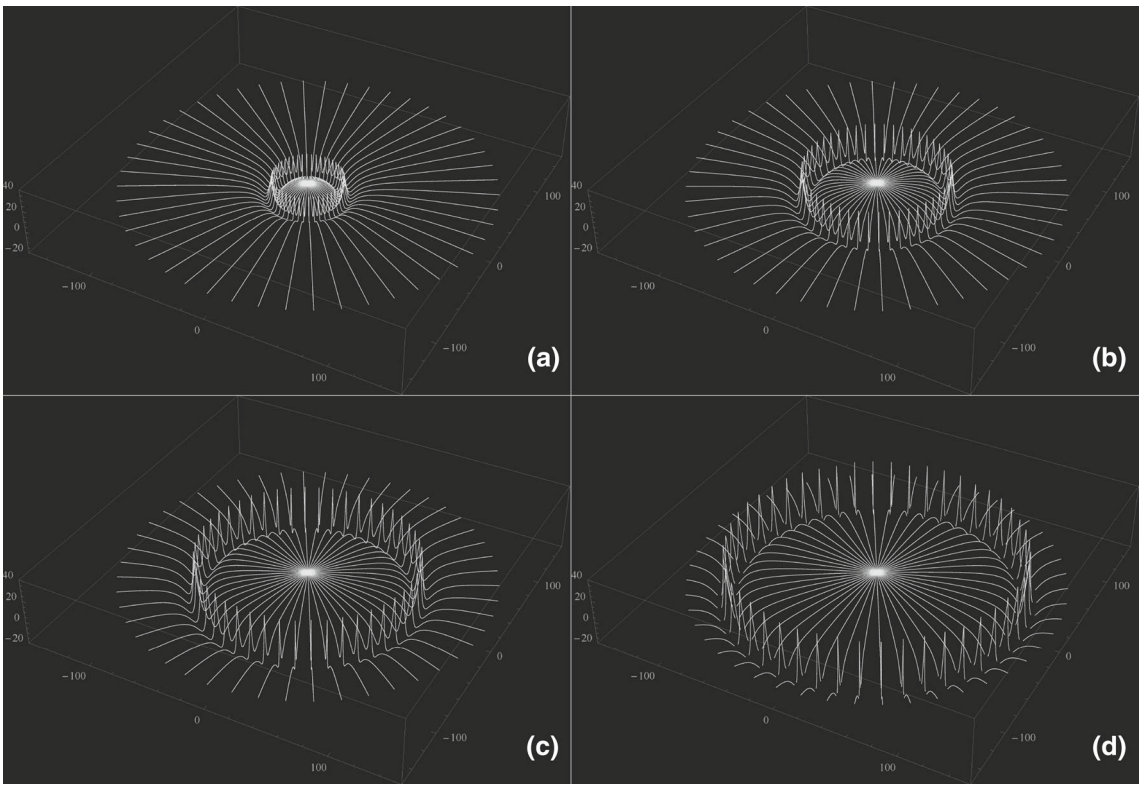

Fig. 7 Contours of perturbed EM fields(electric component) in different positions (30, 60, 90, and 120 m in sub-figures **a**–**d**, respectively) away from the cosmic string, pulse width: 5 m. The accumulation effect is apparent during the propagation of the perturbed EM pulses outward from the symmetric axis

of the given perturbed EM field, but, nonlinearly a smaller width of the GW pulse gives rise to a narrower width of the EM pulse with higher strength of the peak, and a smaller width brings about a greater proportion of the energy being distributed among the high-frequency band (e.g. GHz) in the spectrum. In particular, we find that the perturbed EM pulses propagate at the speed of light, synchronously with the GW pulse, leading to the accumulation effect of their interaction, and it results in growing strength ($\propto \sqrt{\text{distance}}$) of the perturbed EM fields within the region of background magnetic field. These important properties which connect perturbed impulsive EM fields and corresponding GW pulses supports the hypothesis that the obtained solutions are self-consistent and that they reasonably express the inherent physical nature

of the EM response to cylindrical impulsive GW. Clearly, the magnetic component (Eq. (23)) of the perturbed EM field has similar properties.

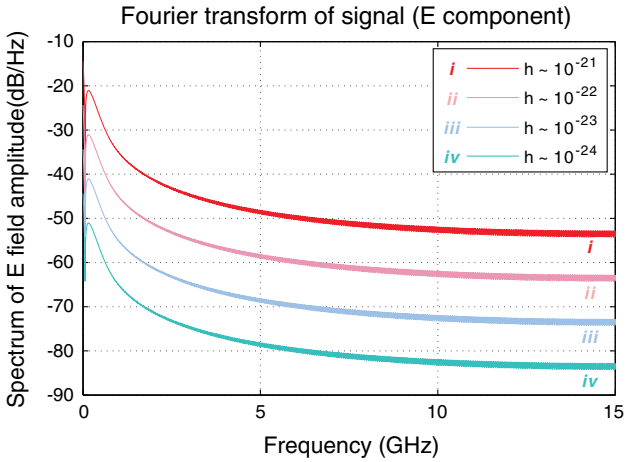

Fig. 8 Amplitude spectra of perturbed EM fields caused by the GW pulses with different amplitudes. This figure demonstrates the amplitude spectra of perturbed EM fields (electric component) caused by the GW pulses with different amplitudes from $\sim 10^{-21}$ to $\sim 10^{-24}$ (with identical width of $a = 0.5$ m). For all cases, the spectra will decay as the frequency grows, but it will still remain at a considerable level even over the GHz band. It reflects the proportional relationship between the overall level of spectrum among all frequency region and the amplitude of GW pulse. The unit 'dB' here means $10 \times log_{10}()$

5 Electromagnetic response to the GW pulse by celestial or cosmological background magnetic fields and its potentially observable effects

The analytical solutions Eqs. (22) and (23) of perturbed EM fields provide helpful information for studying the CSs, impulsive cylindrical GWs, and relevant potentially observable effects. According to classical electrodynamics, the power flux at a receiving surface Δs of the perturbed EM fields may be expressed as

$$U = \frac{1}{2\mu_0} Re[E_y^{(1)*}(x,t) \cdot B_z^{(1)}(x,t)]\Delta s \tag{25}$$

The observability of the perturbed EM fields will be determined concurrently by a lot of parameters of both GW pulse and other observation condition, such as the amplitude and width of the GW pulse, the strength of background magnetic field, the accumulation length (distance from GW source to receiving surface), the detecting technique for weak photons, the noise issue(and so on). Under conditions of current technology, the detectable minimal EM power would be $\sim 10^{-22} W$ in the 1-Hz bandwidth [52], so we could approximately assume the detectable minimal EM power for our case in this paper is the same order of magnitude. Also, the power of the perturbed EM fields is too weak by only using current laboratory magnetic field (e.g., strength of $\sim$20 Tesla, accumulation distance of $=$ 3 m and area of receiving sur-

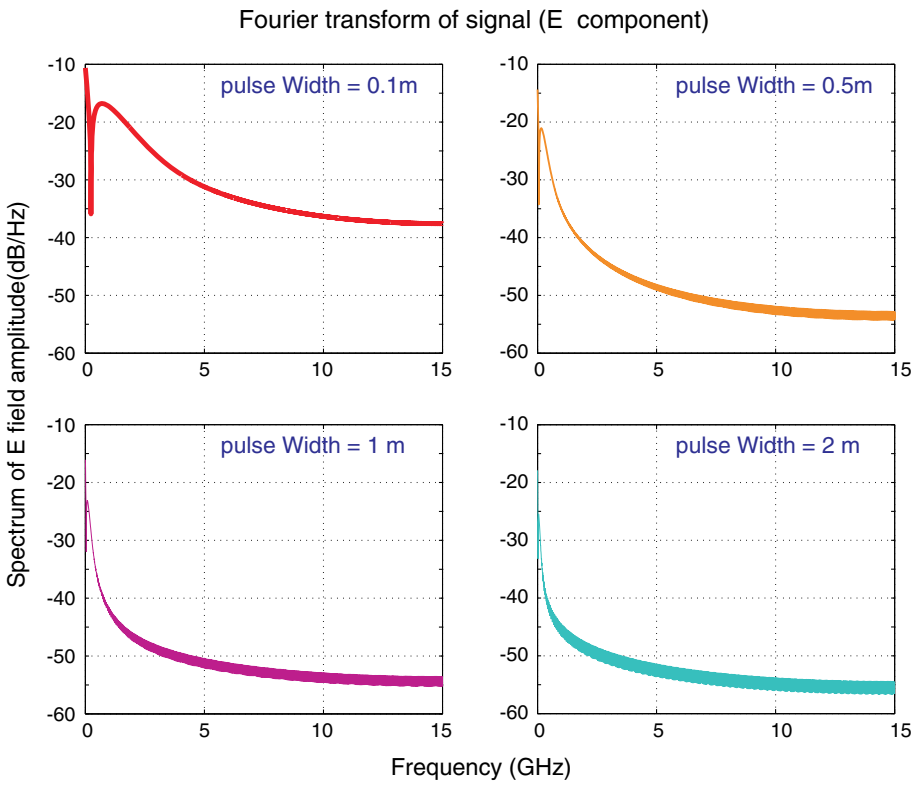

Fig. 9 Amplitude spectra of perturbed EM fields caused by the GW pulses with different widths. In the four subplots involving amplitude spectra of perturbed EM fields, the corresponding GW pulses have different widths of 0.1, 0.5, 1 and 2 m, respectively (all amplitudes are here $\sim 10^{-21}$). It is manifestly obvious that the GW pulse with smaller width (such as 0.1 m), will definitely result in much more energy distributed in the high-frequency bands of the perturbed EM fields. Also, inversely, the GW pulse with larger width (such as 2 m), will lead to conditions for observing a very dramatic attenuation of power of the perturbed EM fields in the high frequency bands. The unit 'dB' here means $10 \times log_{10}()$

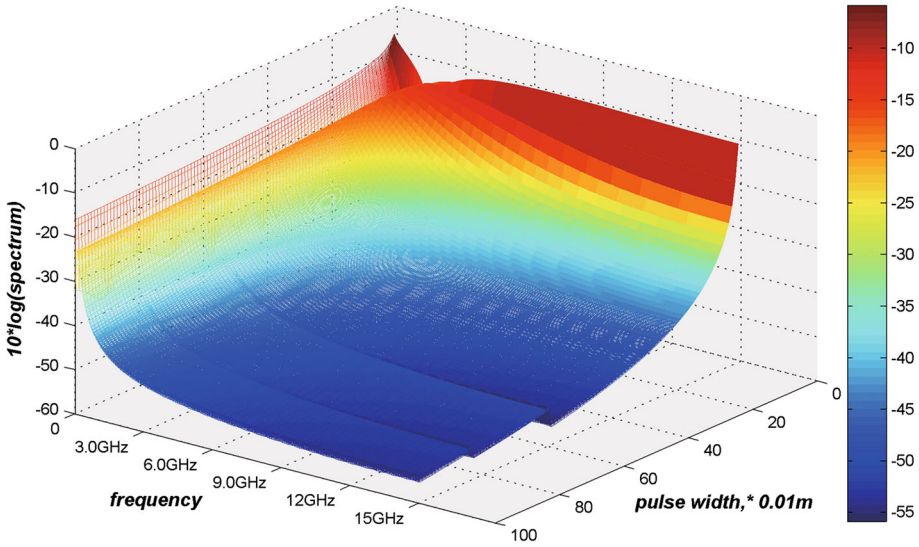

Fig. 10 Continuous contours of amplitude spectra of the perturbed EM fields, caused by GW with different frequency and pulse width. Background magnetic field is set to $B = 10^{11}$ Tesla, and the given amplitude of the GW is set to 10^{-21}. It is obvious that the GW pulse with smaller width will result in richer distribution of energy in high-frequency bands (the area in *red color*)

Table 1 Celestial condition: typical potential ranges of power of the perturbed EM signals, with parameters of amplitude 'h' and width 'a' of the GW pulses. Considering the perturbed EM signals interaction between impulsive cylindrical GWs with extremely high magnetic fields ($\sim 10^{11}$ Tesla) produced by some celestial bodies such as neutron stars [44] (here we denote $B_{SI}^{(0)}$ as background magnetic field in SI units), with the accumulation distance of $\sim$1,000 m and area of receiving surface of Δs $\sim$100 m^2 in the region near axis

Case no.	Signal power (W)	Amplitude h of the GW pulse	Width a of the GW pulse (m)
Celestial condition: $B_{\mathrm{SI}}^{(0)} = 10^{11}$ Tesla, $\Delta s = 100$ m^2, accumulation distance = 1,000			
1	1.15×10^{2}	10^{-21}	0.1
2	1.05×10^{-1}	10^{-21}	1
3	7.78×10^{-5}	10^{-21}	10
4	1.05×10^{-3}	10^{-22}	1
5	1.15×10^{-2}	10^{-23}	0.1

face of $\Delta s = 1.2$ m^2. Note that such a signal will be much less than the minimal detectable EM power of 10^{-22} W). So, for obtaining the power of perturbed EM fields no less than this given minimal detectable level, we would need a very strong background magnetic field (e.g., say a celestial high magnetic field which could reach up to 10^{11} Tesla [44]), or some weak magnetic fields but on an extremely large scale (e.g. a galactic–extragalactic background magnetic field [43], which leads to a significant spatial accumulation effect) are required. These together may permit detection via instrumentation.

In Table 1, we have the conditions of background magnetic fields that are generated by some celestial bodies, such as neutron stars typically. These astrophysical environments could act as natural laboratories. Contemporary research leads us to believe that some young neutron stars can generate extremely high surface magnetic fields of $\sim 10^{10}$ to 10^{11} Tesla [44]. Nevertheless, so far, our knowledge of the exact parameters of the GWs from CSs is still relatively crude (including their amplitude, pulse width, interval between adjacent pulses, and CSs' positions, distribution, spatial scale, etc.), but in keeping with the previous estimation, the GWs from CSs could have an amplitude $\sim 10^{-31}$ or less (in the high-frequency range) in the Earth's region [53]. If we study a specific CS, assuming that the amplitude of the GW emitted by it has the same order of magnitude ($\sim 10^{-31}$ or less) around the globe, then the amplitude of the GW in the region near axis would be roughly $\sim 10^{-21}$ (since the energy flux of cylindrical GW decays as $1/distance$ due to $\tau_0^1 \propto \frac{1}{x}$; see Eq. (33), so the amplitude decays by $1/\sqrt{\text{distance}}$) provided that a possible source of CS would be located somewhere within the Galaxy (e.g., around the center of the Galaxy, about 3000 light years or $\sim 10^{19} m$ away from the globe); or the amplitude of the GW in the region near axis would be roughly $\sim 10^{-20}$, provided that the CS would be located around 1 Mpc ($\sim 10^{22} m$) away. So under this circumstance, if there are very high magnetic fields (e.g., from neutron stars or magnetars) also close to the CS (e.g., around the center of the Galaxy), then the EM response would lead to a quite strong signal with power even up to 10^2 W (see Table I, case 1), which largely surpasses the minimal detectable EM power of $\sim 10^{-22}$ W. However, the method to measure these signals around the magnetars distant from the Earth is still immature, so it would only provide some considerable indirect effect.

On the other hand, the direct observation of expected perturbed EM fields even on the Earth is also possible. The very widely occurring background galactic and extragalactic magnetic fields appearing in all galaxies and galaxy clusters [43] could give a significant contribution to the spatial accumulation effect, during propagating of the GW pulse from its source to the Earth. So, taking this point into considera-

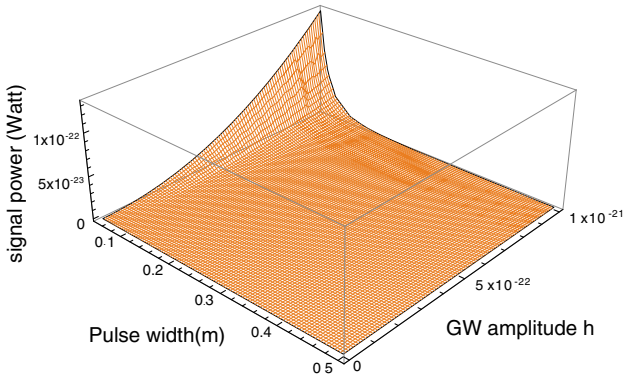

Fig. 11 Continuous 3D plot of the power of perturbed EM fields (in far axis region, around the Earth), by different pulse width and amplitude of the GWs. Here, the background galactic magnetic field is set to 10^{-9} Tesla, the accumulation distance is 2.8×10^{19} m, the area of the receiving surface is 5 m^2

tion, even if the CSs are very far from us, these galactic–extragalactic background magnetic fields (strengths could reach $\sim 10^{-9}$ Tesla within 1 Mpc [43]) will interact with the GW pulses over a huge accumulative distance. Then it would lead to observable signals in the Earth's region, because the accumulation effect of the perturbed EM fields is proportional to $\sqrt{\text{distance}}$ asymptotically ($\sim \sqrt{x}$; see Eq. (28) and Fig. (6)).

For example, as a rough estimation, if we set the accumulation distance $\sim 2.8 \times 10^{19}$ m (e.g. around center of the Galaxy), the GW amplitude $h \sim 10^{-21}$ in the region near axis, the receiving surface $\Delta s \sim 5$ m^2, the GW pulse width $a \sim 5$ cm, and the galactic–extragalactic background magnetic field $B_{\text{GMF}} \sim 10^{-9}$ Tesla, then the power of the signal in the Earth's region would reach up to 1.3×10^{-22} W (see Fig. 11; it already surpasses the minimal detectable EM power of 10^{-22} W, and it means that the photon flux is approximately 112 photons per second in the GHz band). Besides, if this weak signal can be amplified by the schemes of the EM coupling [36,37,54], then a higher signal power would be expected, and the parameters of h, Δs, a, and B_{GMF} would also be enormously relaxed. Still, to extract the amplified signal from the EM coupling system remains a very challenging problem. Moreover, if we consider a larger accumulation distance around 1 Mpc $\sim 10^{22}$ m, with the other parameters $h \sim 10^{-20}$, $\Delta s \sim 1$ m^2, $a \sim 0.1$ m, $B_{\text{GMF}} \sim 10^{-9}$ Tesla [43], then the power of the signal on the Earth would reach up to a magnitude of 1.2×10^{-19} W (which means that the photon flux is about 4.4×10^4 photons per second in the GHz band), which comes with greater direct observability. This EM response, caused by background galactic–extragalactic magnetic fields in all galaxies and galaxy clusters, would also be supplementary to the indirect observation of the GWs interacting with the cosmic microwave background (CMB) radiation [55–59] or some other effects.

6 Asymptotic behaviors

Several representative asymptotic behaviors of the electric component $E_y^{(1)}(x,t)$ of perturbed EM fields (Eq. (22)) can be analytically deduced under diverse conditions, by which way the physical meaning of obtained solution would be expressed more explicitly and simply. In this section we also demonstrate the asymptotic behaviors of the energy density, energy flux density, and Riemann curvature tensor of the impulsive cylindrical GW. The self-consistency, commonalities, and differences among these asymptotic behaviors of both GW pulse and perturbed EM fields will be figured out. For convenience, we use natural units in the whole of this section.

1. Asymptotic behavior of perturbed EM fields in space-like infinite region.
   When the EM pulses propagate in the area where $x \gg t$ and $x \gg a$ (width), from Eq. (22) we have

$$E_y^{(1)}(x,t) \to AB^{(0)}\left[\frac{4t}{x^2} - \frac{12a^2t}{x^4}\right] \propto 4AB^{(0)}\frac{t}{x^2}. \tag{26}$$

   This asymptotic behavior shows that, at a specific time t, $E_y^{(1)}(x,t)$ is weakening fast with respect to the term $1/distance^2$ along the x-axis.
2. Asymptotic behavior of perturbed EM fields in time-like infinite region.
   When the EM pulses propagate in the area where $x \ll t$ and $t \gg a$, also from Eq. (22) we have

$$E_y^{(1)}(x,t) \to AB^{(0)}\frac{4x}{t^2} - 4AB^{(0)}a^2\frac{1}{t^3} \propto 4AB^{(0)}\frac{x}{t^2}. \tag{27}$$

   This asymptotic behavior of $E_y^{(1)}(x,t)$ indicates that, given a specific position x, EM pulses will fade away as $1/t^2$.
3. Asymptotic behavior of perturbed EM fields in light-like infinite region (on the light cone, i.e. $x = t \gg a$).
   As shown in Fig. 12, we define the region having a background magnetic field $B^{(0)}$ is $x \geqslant x_0$, where x_0 is the position of the first contact between wavefront of impulsive GW and $B^{(0)}$, then the interaction duration is from the start time $t_{\min} = 0$, to the end time $t_{\max} = x - x_0 = \Delta x$. In this case, Eq. (22) approaches the form (notice there is a factor c of the light speed in the electric component, but c=1 in the natural units here)

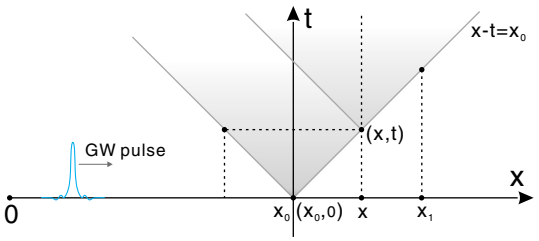

Fig. 12 Asymptotic behavior of the perturbed EM fields in light-like region (on the light cone)

$$E_y^{(1)}(x,t) \to \frac{AB^{(0)}(a^4+4a^2\Delta x^2)^{\frac{1}{4}}}{a^2} \approx \frac{AB^{(0)}[4a^2(x-x_0)^2]^{\frac{1}{4}}}{a^2} \propto \sqrt{x}. \tag{28}$$

Contrary to the E fields in a space-like or time-like infinite region, asymptotically the $E_y^{(1)}(x,t)$ on the light cone will not decay, but will increase, and this particularly reflects the known accumulation effect of the EM response (see Fig. 6 and Sect. 3). It indicates that the light cone is the most interesting area to observe the perturbed EM fields. The magnetic component $B_z^{(1)}(x,t)$ of the perturbed EM fields has similar asymptotic behaviors.

4. Asymptotic behaviors of energy density and energy flux density of the impulsive cylindrical GW.
The expression of the energy density of the impulsive cylindrical GW is [50]

$$\begin{aligned}\tau_0^0 &= \frac{1}{8\pi}e^{2\gamma}(\psi_x^2+\psi_t^2)\\ &= \frac{A^2}{2\pi}\left\{\frac{x^2\cos^2\frac{3}{2}\theta+(t\cos\frac{3}{2}\theta-a\sin\frac{3}{2}\theta)^2}{[x^4+2x^2(a^2-t^2)+(a^2+t^2)^2]^{3/2})}\right\}\\ &\quad\cdot\exp\left\{A^2\left[\frac{1}{a^2}-\frac{2x^2\cos 2\theta}{x^4+2x^2(a^2-t^2)+(a^2+t^2)^2}\right.\right.\\ &\quad\left.\left.-\frac{t^2+a^2-x^2}{a^2[t^4+2t^2(a^2-t^2)+(a^2+t^2)^2]^{1/2}}\right]\right\}.\end{aligned} \tag{29}$$

The expression of energy flux density of impulsive cylindrical GW is [50]

$$\begin{aligned}\tau_0^1 &= -\frac{1}{4\pi}\psi_\rho\psi_t e^{2\gamma}\\ &= \frac{A^2}{2\pi}\left\{\frac{x[2t\cos^2(\frac{3}{2}\theta)-a\sin(3\theta)]}{[x^4+2x^2(a^2-t^2)+(a^2+t^2)^2]^{3/2})}\right\}\\ &\quad\cdot\exp\left\{A^2\left[\frac{1}{a^2}-\frac{2x^2\cos 2\theta}{x^4+2x^2(a^2-t^2)+(a^2+t^2)^2}\right.\right.\\ &\quad\left.\left.-\frac{t^2+a^2-x^2}{a^2[t^4+2t^2(a^2-t^2)+(a^2+t^2)^2]^{1/2}}\right]\right\}\end{aligned}$$

$$\text{where } \theta=\theta_1=\arctan\frac{2at}{x^2+a^2-t^2}. \tag{30}$$

So we find that:

(i) In the space-like infinite region, where $x \gg t$ and $x \gg a$, we have the asymptotic behaviors of the energy density and energy flux density of the impulsive cylindrical GW as follows:

$$\tau_0^0 \to \frac{A^2}{2\pi}\left(\frac{1}{x^4}+\frac{t^2}{x^6}\right)\exp\left(\frac{2A^2}{a^2}\right) \to O(x^{-4}),$$
$$\tau_0^1 \to \frac{A^2t}{\pi x^5}\exp\left(\frac{2A^2}{a^2}\right) \to O(x^{-5}), \tag{31}$$

where the energy density and the energy flux density fall off very quickly as the distance x rises.

(ii) In the time-like infinite region, where $t \gg x$ and $t \gg a$, we have the asymptotic behavior of energy density and energy flux density:

$$\tau_0^0 \to \frac{A^2}{2\pi t^4}\exp\left(-\frac{2A^2x^2}{t^4}\right) \to O(t^{-4}),$$
$$\tau_0^1 \to \frac{A^2x}{\pi t^5}\exp\left(-\frac{2A^2x^2}{t^4}\right) \to O(t^{-5}), \tag{32}$$

where the energy density and energy flux density also drop rapidly as the time increases.

(iii) In light-like infinite region (on the light cone, where $x=t \gg a$, as the most physically interesting region), their asymptotic behaviors are

$$(\tau_0^0)_{x=t\gg a} \to \frac{A^2}{16\pi a^3x}\exp\left(\frac{3A^2}{2a^2}\right) \propto \frac{1}{x},$$
$$(\tau_0^1)_{x=t\gg a} \to \frac{A^2}{16\pi a^3x}\exp\left(\frac{3A^2}{2a^2}\right) \propto \frac{1}{x}. \tag{33}$$

Therefore, the energy density and energy flux density here decay much more slowly on the light cone, compared to those in space-like or time-like infinite regions. These asymptotic behaviors are consistent to the asymptotic behaviors of the perturbed EM fields shown above.

5. Asymptotic behaviors of the Riemann curvature tensor of the impulsive cylindrical GW. We chose two typical non-vanishing components R_{xzxz} and R_{y0y0} of covariant curvature tensor, and they have the forms [50]

$$R_{xzxz} = e^{2\psi}(-\psi_t\gamma_t+\psi_t^2-\psi_x\gamma_x+\psi_{xx})$$

$$= \mathrm{e}^{2\psi}\left\{\frac{-2A\cos\frac{3}{2}\theta}{r^{3/4}}+\frac{6Ax^2\cos\frac{5}{2}\theta}{r^{5/4}}\right.$$
$$+\frac{16A^3x^2\cos\frac{3}{2}\theta\left[x^2\cos^2\frac{3}{2}\theta+2(x\cos\frac{3}{2}\theta-a\sin\frac{3}{2}\theta)^2\right]}{r^{9/4}}$$
$$\left.+\frac{4A^2\left[2x^2\cos^2\frac{3}{2}\theta+(x\cos\frac{3}{2}\theta-a\sin\frac{3}{2}\theta)^2\right]}{r^{3/2}}\right\}, \quad (34)$$

where $r = x^4 + 2x^2(a^2 - t^2) + (a^2 + t^2)^2$, the same hereinafter, and

$$R_{y0y0}$$
$$= -\mathrm{e}^{-2\psi}(-\psi_{tt} - \psi_t\gamma_t + (\gamma_x - \psi_x)/x - \psi_x\gamma_x + \psi_x^2)$$
$$= -\mathrm{e}^{-2\psi}\left\{\frac{4A\cos\frac{3}{2}\theta}{r^{3/4}}+\frac{6A\left[(t^2-a^2)\cos\frac{5}{2}\theta-at\sin\frac{5}{2}\theta\right]}{r^{5/4}}\right.$$
$$-\frac{8A^3x^2\cos^2\frac{3}{2}\theta\left[x^2\cos^2\frac{3}{2}\theta-(t\cos\frac{3}{2}\theta-a\sin\frac{3}{2}\theta)^2\right]}{r^{9/4}}$$
$$\left.+\frac{4A^2\left[2x^2\cos^2\frac{3}{2}\theta+(t\cos\frac{3}{2}\theta-a\sin\frac{3}{2}\theta)^2\right]}{r^{3/2}}\right\}, \quad (35)$$

then we find that:

(i) in the space-like infinite region where $x \gg t$ and $x \gg a$, asymptotically it gives

$$R_{xzxz} \to \left(\frac{4A}{x^3}+\frac{12A^2}{x^4}+\frac{48A^3}{x^5}\right)\exp\left(\frac{4A}{x}\right)$$
$$\to \frac{4A}{x^3}\exp\left(\frac{4A}{x}\right)\to O\left(\frac{1}{x^3}\right) \quad (36)$$

and

$$R_{y0y0} \to -\left[\frac{4A}{x^3}+\frac{8A^2}{x^4}+\frac{6A(t^2-a^2)-8A^3}{x^5}\right]$$
$$\times\exp\left(\frac{-4A}{x}\right)$$
$$\to \frac{-4A}{x^3}\exp\left(\frac{-4A}{x}\right)\to O\left(\frac{1}{x^3}\right); \quad (37)$$

(ii) in the time-like infinite region, where $t \gg x$ and $t \gg a$, we have the asymptotic behaviors

$$R_{xzxz} \to \left(\frac{-2A}{t^3}+\frac{6Ax^2}{t^5}+\frac{12A^2x^2}{t^6}+\frac{48A^3x^4}{t^9}\right)$$
$$\times\exp\left(\frac{4A}{t}\right)$$
$$\to \frac{-2A}{t^3}\exp\left(\frac{4A}{t}\right)\to O\left(\frac{1}{t^3}\right) \quad (38)$$

and

$$R_{y0y0} \to \left(\frac{10A}{t^3}+\frac{4A^2}{t^4}+\frac{8A^3x^2}{t^7}\right)$$
$$\times\exp\left(\frac{-4A}{t}\right)$$
$$\to \frac{-10A}{t^3}\exp\left(\frac{-4A}{t}\right)\to O\left(\frac{1}{t^3}\right); \quad (39)$$

(iii) in the light-like infinite region (on the light cone), where $x = t \gg a$, their asymptotic behaviors are

$$R_{xzxz} \to -\frac{3}{4}\left(\frac{A}{a^{5/2}x^{1/2}}+\frac{A^3}{a^{9/2}x^{1/2}}\right)$$
$$\times\exp\left(\frac{-2A}{a^{1/2}x^{1/2}}\right)\propto\frac{1}{x^{1/2}} \quad (40)$$

and

$$R_{y0y0} \to \left(\frac{3A}{4a^{5/2}x^{1/2}}+\frac{3A^2}{4a^3x}+\frac{A}{a^{3/2}x^{3/2}}\right)$$
$$\times\exp\left(\frac{2A}{a^{1/2}x^{1/2}}\right)$$
$$\to \frac{3A}{4a^{5/2}x^{1/2}}\exp\left(\frac{2A}{a^{1/2}x^{1/2}}\right)\propto\frac{1}{x^{1/2}}. \quad (41)$$

Apparently, these components of the Riemann curvature tensor decrease much more slowly on the light cone (the most interesting region and the particular one with the richest observable information), as compared to those in the space-like or time-like infinite regions where they attenuate very rapidly. This characteristic agrees well with the asymptotic behaviors of the energy density, energy flux density of the impulsive cylindrical GW, and asymptotic behaviors of the perturbed EM fields. Particularly, only on the light cone, the perturbed EM fields will be growing instead of declining, which specially reflects the spatial accumulation effect. All of the above asymptotic behaviors play supporting roles in further corroboration of the self-consistency and reasonableness of the obtained solutions.

7 Conclusion and discussion

First, in the frame of general relativity, based upon the electrodynamical equations in curved spacetime, utilizing the d'Alembert formula and relevant approaches, the analytical solutions $E_y^{(1)}(x,t)$ and $B_z^{(1)}(x,t)$ of the impulsive EM fields, perturbed by cylindrical GW pulses (which could be emitted from cosmic strings) propagating through a background magnetic field are obtained. It is shown that the perturbed EM fields are also in the impulsive form, consistent with the impulsive cylindrical GWs, and the solutions can

naturally give the accumulation effect of perturbed EM signal (due to the fact that perturbed EM pulses propagate at the speed of light synchronously with the propagating GW pulse), by the term of the square root of the accumulated distance, i.e. $\propto \sqrt{\text{distance}}$. Based on this accumulation effect, we for the first time predict a possible directly observable effect ($\geq 10^{-22}$ W, stronger than the minimal detectable EM power under current experimental condition) on the Earth caused by the EM response of the GWs (from CSs) interacting with background galactic–extragalactic magnetic fields.

Second, asymptotic behaviors of the perturbed EM fields are accordant to asymptotic behaviors of the GW pulse and some of its relevant physical quantities such as energy density, energy flux density and Riemann curvature tensor, and it brings cogent affirmation supporting the self-consistency and reasonableness of the obtained solutions. Asymptotically, almost all of these physical quantities will decrease once the distance grows, and these physical quantities decrease much more slowly on the light cone (in the light-like region), which is the most interesting area with the richest physical information, rather than the asymptotic behaviors in the space-like or time-like regions where they attenuate rapidly. However, only perturbed EM fields in the light cone will not decrease, but, instead, increase. Also, we find that the asymptotic behaviors of perturbed EM fields particularly reflect the profile and dynamical behavior of the spatial accumulation effect.

Third, perturbed EM fields caused by the cylindrical impulsive GWs from CSs are often very weak, and then direct detection or indirect observation would be very difficult on the Earth. However, many contemporary research results convince us that there are extremely high magnetic fields in some celestial bodies' regions (such as neutron stars [44], which could cause indirect observable effects), and very widely distributed galactic–extragalactic background magnetic fields in all galaxies and galaxy clusters [43]; and especially the latter might provide a huge spatial accumulation effect for the perturbed EM fields, and they would lead to very interesting and potentially observable effects in the Earth's region (as to the effect for direct observation; see Sect. 5), even if such CSs are distant from the Earth (e.g., located around the center of the Galaxy, i.e., about 3,000 light years away, or even further, like $\sim$1 Mpc).

In addition we find that the analysis of the representative physical properties of the perturbed EM fields also reveals that: (1) The amplitude of the GW pulse proportionally influences the level and overall spectrum of the perturbed EM field. (2) The smaller width of the GW pulse nonlinearly gives rise to narrower widths, higher peaks of the perturbed EM pulses, and a greater proportion of energy distributed in the high-frequency band (e.g. GHz) in the amplitude spectra of the perturbed EM fields.

According to previous studies, the cylindrical GWs from CSs include both impulsive and usual continuous forms. Specially, in this paper we only focus on the impulsive case due to its concentrated energy, the pre-existing rigorous metric (Einstein–Rosen metric), and its impulsive property to give the rich GW components covering a wide frequency band, etc. Nevertheless, the EM response to the usual continuous GWs also would bring about meaningful information and have value for an in-depth study in future. Moreover, in order to enhance the real detectability of the perturbed EM fields, various considerable improvements could be introduced, such as EM coupling [36,37,60,61] and also the use of superconductivity cavity technology [54]. We intend to make thorough investigations of these additional research topics in the future.

Acknowledgments This work is supported by the National Nature Science Foundation of China No.11375279, the Foundation of China Academy of Engineering Physics No.2008 T0401 and T0402.

References

1. BICEP2 Collaboration. arXiv:1403.3985v2
2. B. Allen. arXiv:gr-qc/9604033
3. A. Vilenkin, Phys. Lett. B **107**, 47 (1981)
4. R.R. Caldwell, B. Allen, Phys. Rev. D **45**, 3447 (1992)
5. T. Vachaspati, A. Vilenkin, Phys. Rev. D **31**, 3052 (1985)
6. C.J. Hogan, M.J. Rees, Nature **311**, 109 (1984)
7. T. Damour, A. Vilenkin, Phys. Rev. Lett. **85**, 3761 (2000)
8. T. Damour, A. Vilenkin, Phys. Rev. D **71**, 063510 (2005)
9. L. Leblond, B. Shlaer, X. Siemens, Phys. Rev. D **79**, 123519 (2009)
10. J.F. Dufaux, D.G. Figueroa, J. García-Bellido, Phys. Rev. D **82**, 083518 (2010)
11. V. Berezinsky, B. Hnatyk, A. Vilenkin, Phys. Rev. D **64**, 043004 (2001)
12. E.J. Copeland, R.C. Myers, J. Polchinski, J. High Energy Phys. **06**, 013 (2004)
13. X. Siemens, J. Creighton, I. Maor, S.R. Majumder, K. Cannon, J. Read, Phys. Rev. D **73**, 105001 (2006)
14. J. Podolský, J.B. Griffiths, Class. Quantum Grav. **17**, 1401 (2000)
15. J. Podolský, R. Švarc, Phys. Rev. D **81**, 124035 (2010)
16. R. Gleiser, J. Pullin, Class. Quantum Grav. **6**, L141 (1989)
17. R.J. Slagter, Class. Quantum Grav. **18**, 463 (2001)
18. M. Hortaçsu, Class. Quantum Grav. **13**, 2683 (1996)
19. R. Steinbauer, J.A. Vickers, Class. Quantum Grav. **23**, R91 (2006)
20. F. Dubath, J.V. Rocha, Phys. Rev. D **76**, 024001 (2007)
21. S. Ölmez, V. Mandic, X. Siemens, Phys. Rev. D **81**, 104028 (2010)
22. P. Patel, X. Siemens, R. Dupuis, J. Betzwieser, Phys. Rev. D **81**, 084032 (2010)
23. K. Kleidis, A. Kuiroukidis, P. Nerantzi, D. Papadopoulos, Gen. Relat. Gravit. **42**, 31 (2010)
24. M.B. Hindmarsh, T.B.W. Kibble, Rep. Progr. Phys. **58**, 477 (1995)
25. A. Vilenkin, E.P.S. Shellard, *Cosmic Strings and Other Topological Defects* (Cambridge University Press, Cambridge, 2000)
26. A. Wang, N.O. Santos, Class. Quantum Grav. **13**, 715 (1996)
27. R. Gregory, Phys. Rev. D **39**, 2108 (1989)

28. B.P. Abbott et al., Phys. Rev. D **80**, 062002 (2009)
29. X. Siemens, V. Mandic, J. Creighton, Phys. Rev. Lett. **98**, 111101 (2007)
30. P.P. Binétruy, A. Bohée, T. Hertog, D.A. Steer, Phys. Rev. D **82**, 126007 (2010)
31. M.I. Cohen, C. Cutler, M. Vallisneri, Class. Quantum Grav. **27**, 185012 (2010)
32. E. O'Callaghan, S. Chadburn, G. Geshnizjani, R. Gregory, I. Zavala, Phys. Rev. Lett. **105**, 081602 (2010)
33. D.P. Bennett, F.R. Bouchet, Phys. Rev. Lett. **60**, 257 (1988)
34. R.R. Caldwell, R.A. Battye, E.P.S. Shellard, Phys. Rev. D **54**, 7146 (1996)
35. S. Sarangi, S. Tye, Phys. Lett. B **536**, 185 (2002)
36. F.Y. Li, M.X. Tang, D.P. Shi, Phys. Rev. D **67**, 104008 (2003)
37. F.Y. Li, R.M.L. Baker Jr, Z.Y. Fang, G.V. Stepheson, Z.Y. Chen, Eur. Phys. J. C **56**, 407 (2008)
38. F.Y. Li, N. Yang, Z. Fang, R.M.L. Baker, G.V. Stephenson, H. Wen, Phys. Rev. D **80**, 064013 (2009)
39. W.K. De Logi, A.R. Mickelson, Phys. Rev. D **16**, 2915 (1977)
40. D. Boccaletti, V. De Sabbata, P. Fortint, C. Gualdi, Nuovo Cim. B **70**, 129 (1970)
41. A. Einstein, N. Rosen, J. Franklin Inst. **223**, 43 (1937)
42. N. Rosen, Physik Z. Sowjetunion **12**, 366 (1937)
43. L.M. Widrow, Rev. Mod. Phys. **74**, 775 (2002)
44. B.D. Metzger, T.A. Thompson, E. Quataert, Astrophys. J. **659**, 561 (2007)
45. J. Weber, General Relativity And Gravitational Waves. *Dover Books on Physics Series* (Dover Publications, New York, 1961)
46. J. Weber, J.A. Wheeler, Rev. Mod. Phys. **29**, 509 (1957)
47. N. Rosen, K.S. Virbhadra, Gen. Rel. Grav. **25**, 429 (1993)
48. N. Rosen, Heiv. Phys. Acta Suppl IV, 171 (1956)
49. N. Rosen, Phys. Rev. **110**, 291 (1958)
50. F.Y. Li, M.X. Tang, Acta Phys. Sin. **6**, 321 (1997)
51. A.N. Tikhonov, A.A. Samarskii, in *Equations of Mathematical Physics, Dover Books on Physics*, ed. by D.M. Brink, Chap. II-2-7 (Dover publications Inc, New York, 2011), p. 73, dover ed
52. A.M. Cruise, Class. Quantum Grav. **29**, 095003 (2012)
53. B.P. Abbott et al., Nature (London) **460**, 990 (2009)
54. F.Y. Li, Y. Chen, P. Wang, Chin. Phys. Lett. **24**, 3328 (2007)
55. D. Baskaran, L.P. Grishchuk, A.G. Polnarev, Phys. Rev. D **74**, 083008 (2006)
56. B.G.K.A.G. Polnarev, N.J. Miller, Month. Not. R. Astronom. Soc. **386**, 1053 (2008)
57. U. Seljak, M. Zaldarriaga, Phys. Rev. Lett. **78**, 2054 (1997)
58. J.R. Pritchard, M. Kamionkowski, Ann. Phys. (N.Y.) **318**, 2 (2005)
59. W. Zhao, Y. Zhang, Phys. Rev. D **74**, 083006 (2006)
60. J. Li, K. Lin, F.Y. Li, Y.H. Zhong, Gen. Relativ. Gravit. **43**, 2209 (2011)
61. R. Woods et al., J. Mod. Phys. **2**, 498 (2011)